



RESEARCH ARTICLE

Kilowatt-level supercontinuum generation in a single-stage random fiber laser with a half-open cavity

Li Jiang^{1,2,3}, Jinming Wu^{1,2,3}, Rui Song^{1,2,3}, Zilun Chen^{1,2,3}, Xiran Zhu^{1,2,3}, Fengchang Li^{1,2,3}, Kailong Li^{1,2,3}, Hanwei Zhang^{1,2,3}, and Jing Hou^{1,2,3}

¹College of Advanced Interdisciplinary Studies, National University of Defense Technology, Changsha, China

²Nanhu Laser Laboratory, National University of Defense Technology, Changsha, China

³Hunan Provincial Key Laboratory of High Energy Laser Technology, National University of Defense Technology, Changsha, China

(Received 14 May 2023; revised 17 July 2023; accepted 8 August 2023)

Abstract

The random distributed-feedback fiber laser (RFL) is a new approach to obtain a high-power stable supercontinuum (SC) source. To consider both structure simplification and high-power SC output, an innovative structure achieving a kilowatt-level SC output in a single-stage RFL with a half-open cavity is demonstrated in this paper. It consists of a fiber oscillator, a piece of long passive fiber and a broadband coupler, among which the broadband coupler acting as a feedback device is crucial in SC generation. When the system has no feedback, the backward output power is up to 298 W under the pump power of 1185 W. When the feedback is introduced before the pump laser, the backward power loss can be reduced and the pump can be fully utilized, which could promote forward output power and conversion efficiency significantly. Under the maximum pump power of 1847 W, a 1300 W SC with spectrum ranging from 887 to 1920 nm and SC conversion efficiency of 66% is obtained. To the best of our knowledge, it is the simplest structure used for high-power SC generation, and both the generated SC output power and the conversion efficiency are highest in the scheme of the half-opened RFL output SC.

Keywords: high conversion efficiency; high-power supercontinuum; random fiber laser; single-stage structure

1. Introduction

The supercontinuum (SC), with rich spectral compositions and laser properties, has experienced rapid growth since photonic crystal fiber (PCF) was developed in 1996^[1]. As a research hotspot of the SC, the high-power SC has received great attention due to its applications in hyperspectral lidar, optoelectronic countermeasures and astronomical optical frequency combs^[2,3]. As a nonlinear medium used for SC generation, PCF with a small core size is not conducive to the scaling of SC output power^[4], but large mode area (LMA) fiber is an appropriate choice. At present, the major scheme used for high-power SC generation based on LMA fiber is to employ the main oscillation power amplifier structure^[5,6]. However, this scheme has not only a complex structure, but also the risk of laser damage due to improper operation,

such as the self-excited oscillation caused by the amplified spontaneous emission.

SC generation in a single-stage structure can not only lower the cost and the packaging difficulty, but also reduce the security risks. In 2022, a 791 W SC ranging from 1000 to 1500 nm was realized in a quasi-continuous wave fiber oscillator. However, the spectral performance is not ideal even at the high peak pump of 34 kW^[7]. Compared with this scheme, the random distributed-feedback fiber laser (RFL) consisting of a continuous wave (CW) fiber oscillator has a simpler structure with unique features, such as low background noise and sound robustness, and is free of the photon darkening effect^[8]. The output power of the near-single-mode fiber oscillator reached 8 kW in 2020^[9], which lays the foundation for the realization of the single-stage high-power RFL. Based on a fiber oscillator, single-wavelength kilowatt-level RFLs with a half-open cavity and a full-open cavity have been reported^[10,11]. In 2022, a kilowatt RFL with a full-open cavity was demonstrated experimentally^[11]. A short passive fiber length is crucial in this

Correspondence to: Rui Song and Jing Hou, College of Advanced Interdisciplinary Studies, National University of Defense Technology, Changsha 410073, China. Emails: srnotice@163.com (R. Song); hou-jing25@sina.com (J. Hou)

point-reflector-free RFL to enable a one-direction output due to the reduced accumulation of backward Rayleigh scattering light, only set to 35 m in the experiment. However, in SC generation, a long fiber is required to obtain sufficient nonlinear accumulation, especially under the condition of CW pumping. Controlling the backward Rayleigh scattered light is key to gain a high-power SC with unidirectional output in a single-stage RFL. Taking the above into account, the introduction of a feedback device is applicable to obtain a high-power SC with unidirectional output. Commonly, the feedback device is placed between the pump laser and the passive fiber to feed the backward Rayleigh scattered light to the forward direction. The broadband feedback is provided by a broadband mirror, coupler or fiber end feedback, and a wavelength division multiplexer (WDM) is included to act as a bridge^[12–15]. This means that the WDM needs to withstand the high pump injecting, which also increases the complexity of the system simultaneously. Based on this scheme, the maximum SC output power in a single-stage RFL was maintained at about 40 W^[12]. Further power scaling is limited by the high-power processing capacity of the WDM.

In this paper, we propose an innovative structure to obtain kilowatt-level SC output based on a single-stage RFL with a half-open cavity. The broadband feedback is introduced by adding a broadband coupler before the pump laser, which is more conducive to scale the SC output power and enhance the SC conversion efficiency compared with feedback introduced after the pump laser. The random distributed feedback and the nonlinear accumulation are provided by a piece of long passive fiber. By contrast, SC output performances in the system without feedback are demonstrated. The results indicate that when the feedback is introduced, both the SC output power and the conversion efficiency have been apparently improved. Under the maximum pump power of 1847 W, a 1300 W SC with spectral range of 887–1920 nm and conversion efficiency of 66% is obtained.

2. Experimental setup

Figure 1 shows the experimental setup for kilowatt-level SC generation. It is formed in a single-stage RFL with

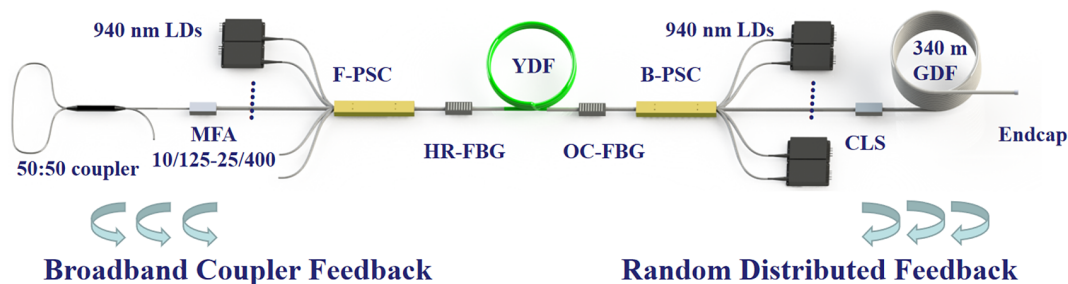


Figure 1. Experimental scheme for kilowatt-level SC generation in a single-stage RFL with a half-open cavity. MFA, mode field adapter; HR-FBG, high-reflectivity fiber Bragg grating; F-PSC, forward pump/signal combiner; YDF, ytterbium-doped fiber; OC-FBG, output coupler fiber Bragg grating; B-PSC, backward pump/signal combiner; LD, laser diode; CLS, cladding light stripper; GDF, germanium-doped fiber.

a half-open cavity. Specifically, the pump source used for bidirectionally pumping the fiber oscillator consists of 27 laser diodes (LDs) with central wavelength of 940 nm. The fiber oscillator has a central wavelength of 1080 nm and acts as the pump laser for SC generation. Both the forward and backward $(18 + 1) \times 1$ pump/signal combiners are used to couple the pump into a piece of 25/400 μm ytterbium-doped fiber (YDF) with a low pump absorption coefficient of 0.56 dB/m at 915 nm and a fiber length of 35 m. A pair of fiber Bragg gratings (FBGs) are placed on either side of the LMA YDF to form a resonant cavity, where the reflectivity of the high-reflectivity fiber Bragg grating (HR-FBG) and that of the output coupler fiber Bragg grating (OC-FBG) are 99.9% and 6.2% with 3 dB bandwidths of 4 and 1 nm, respectively. Two separate cladding light strippers (CLSs) could effectively remove the residual cladding light. A 10/125 μm coupler with power ratio of 50:50 and working wavelength of 1160 ± 40 nm is used for broadband feedback, which is connected to the system with the help of a 10/125–25/400 μm mode field adapter (MFA). A piece of 25/400 μm germanium-doped fiber (GDF) with a fiber length of 340 m is used to provide random distributed feedback and nonlinear accumulation. A homemade endcap is cleaved at an angle of 8° to avoid end feedback. The whole system of the fiber oscillator is fixed on a water-cooled plate, and the long GDF is coiled in a water-cooled bucket. The coupler and MFA are placed on an aluminum plate for heat dissipation, and their temperatures are monitored by a thermal infrared viewer.

3. Results and discussion

3.1. Single-stage RFL with a full-open cavity

The output spectrum of the SC was collected by two optical spectrum analyzers (Yokogawa, AQ6374 and AQ6375) with spectral bands of 350–1750 and 1200–2400 nm, respectively. The measured spectra were spliced together by aligning the spectral intensity.

Firstly, the broadband coupler is removed and the idle fiber output end of the HR-FBG is cleaved at an angle of 8° to prevent end feedback. The output end of the HR-FBG

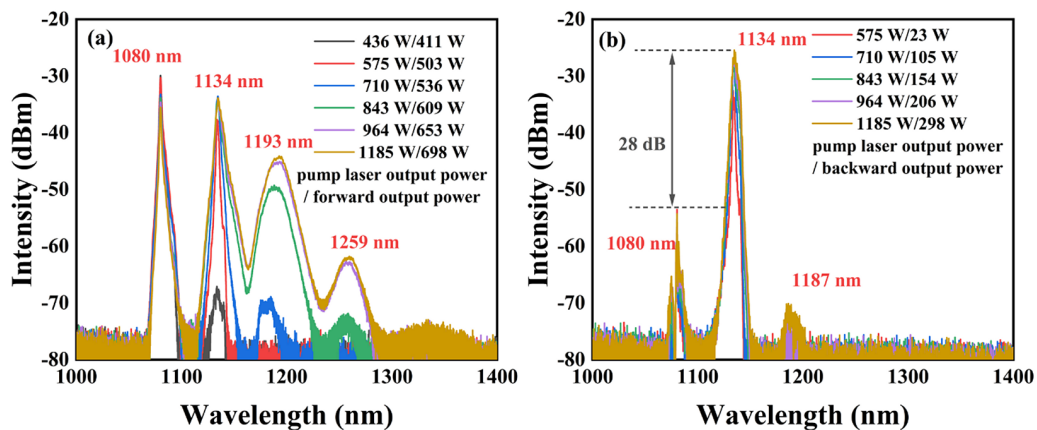


Figure 2. Output spectral evolution of pump laser power in the RFL with a full-open cavity: (a) forward direction and (b) backward direction.

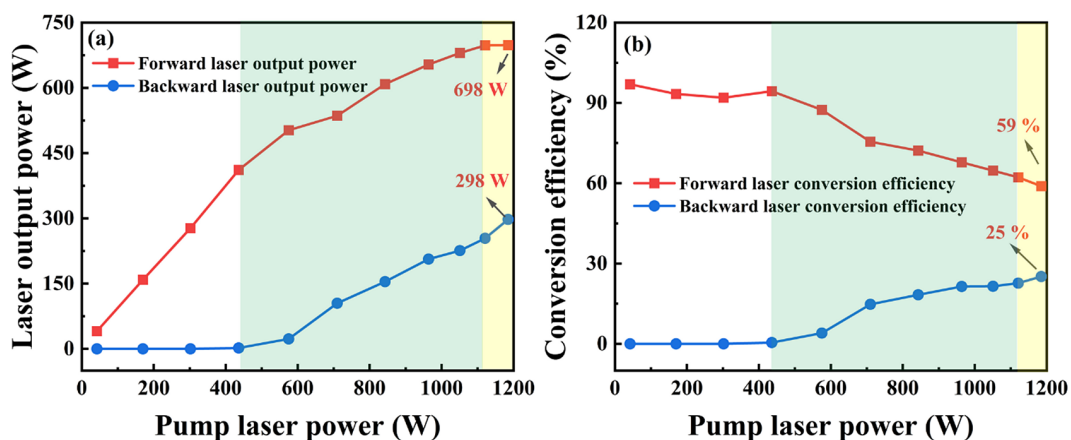


Figure 3. (a) Laser output power and (b) conversion efficiency of the RFL with a full-open cavity in both directions. The green background area is the growth area of the backward output power; the yellow background area shows that the forward output power stops increasing.

is defined as the backward output direction. The output performances of the RFL with a full-open cavity are measured. The spectral evolutions of the forward and backward output laser are recorded in Figure 2. The zero-dispersion wavelengths (ZDWs) of 25/400 μm YDF and GDF are about 1.3 μm . When the pump is located in the normal dispersion region of the fiber, the Raman effect dominates the initial spectrum expansion^[16]. The spectrum of Figure 2(a) shows three Raman peaks at the maximum pump power, which lie around 1134, 1193 and 1259 nm, and they all correspond to a 13.2 THz downshift of the previous signal wavelength. The higher-order Raman peak has the larger spectral bandwidth, benefiting from the broadband Raman gain spectrum of the Raman effect^[17]. For the backward output spectrum in Figure 2(b), the intensity of the 1134 nm first-order Raman peak is about 28 dB higher than that of the pump peak, which indicates that the backward output laser is basically concentrated in the first-order Raman peak.

The forward and backward laser output powers are measured to quantitatively observe the laser output performance. Figure 3(a) plots the laser output powers versus the pump

laser power in the forward and backward directions, and corresponding conversion efficiencies are shown in Figure 3(b). At first, the forward laser output power increases almost linearly with the injecting of the pump laser. When the pump laser power reaches 575 W, the forward laser output power reaches the threshold for backward Rayleigh scattering, and the backward laser starts to appear. The backward laser obtains the active gain when it passes through the YDF, which is because the wavelength of the backward laser (1134 nm) is located in the ytterbium ion radiation range of 1000–1200 nm. With the pump laser power increasing to 1185 W, the backward output power is amplified to 298 W with the aid of the distributed Raman gain and the active gain. In this process of power scaling, the conversion efficiency of the forward laser decreases. The forward first-order Raman laser and the pump laser have opposite intensity distributions along the GDF, resulting in the saturation of forward first-order Raman gain. The Raman gain saturation becomes increasingly obvious with the increase of the pump laser power^[18]. As the pump laser power reaches the maximum value, the conversion efficiency of the forward laser

descends to 59% and the forward output power almost stops growing. This is caused by the combination effect of the Raman gain saturation of the forward laser and the quantum defect occurring in the process of wavelength conversion in the forward direction. In Ref. [18], the backward first-order Raman output power always is higher than the forward first-order Raman output power due to the Raman gain saturation of the forward laser. However, in our full-opened RFL at the maximum pump laser power, the calculated forward and backward first-order Raman output powers by the method of spectral integration are 443 and 294 W, respectively. The lower backward first-order Raman output power is due to insufficient distributed backward scattering and the existence of the walk-off effect^[11]. If further increasing the pump laser power, the energy pump may be completely transferred to the backward output laser due to the enhanced backward scattering, the Raman gain saturation of the forward laser and the quantum defect in the forward direction.

3.2. Single-stage RFL with a half-open cavity

It can be seen from the discussion above that the backward output power is rather high in the single-stage RFL with a full-open cavity. To solve this problem, a broadband coupler is installed before the pump laser to form a half-opened RFL. It is noted that in the RFL with a full-open cavity, the strong backward laser is obtained by the weak backward Rayleigh scattering light combined with the distributed Raman gain and ytterbium ion active gain. When the coupler is added, gain competition occurs between the forward feedback light and the weak backward Rayleigh scattered light in the transmission process along the fiber. Part of the energy is transferred to the forward laser and the backward output power is reduced, which means that the coupler does not need to withstand too much power. It is roughly estimated by monitoring the coupler temperature and the result shows that the temperature of the coupler has no obvious rise in the whole process of power scaling. Figure 4 shows the compared output spectra of RFLs with a full-open cavity and a half-open cavity under the same pump power of 964 W. The inset displays the forward and backward output power in both structures. The results demonstrate that the backward output light is fed back into the forward direction with the aid of the broadband coupler, promoting forward output power and conversion efficiency. The output spectrum of the half-opened RFL is greatly expanded compared to that of the full-opened RFL under the same pump power. This is because the boosting of forward output power facilitates the interaction among nonlinear effects, such as the Raman effect, phase-matched four-wave mixing and group-velocity-matched dispersive wave, thus promoting the conversion among wavelengths.

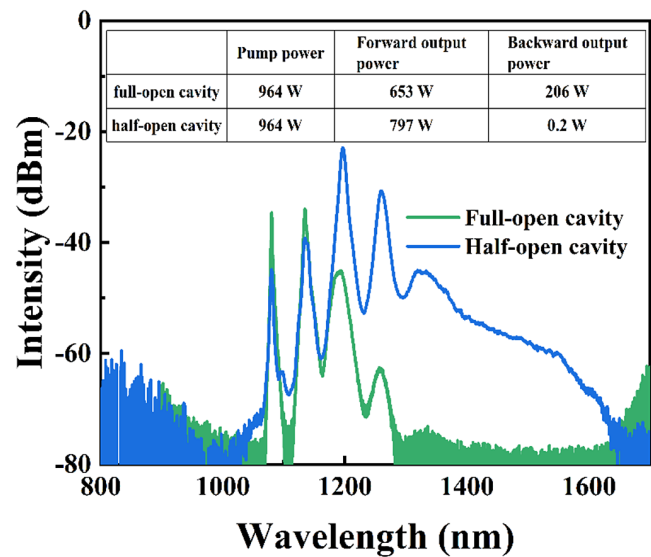


Figure 4. Compared output spectra of RFLs with a full-open cavity and a half-open cavity under the same pump power of 964 W.

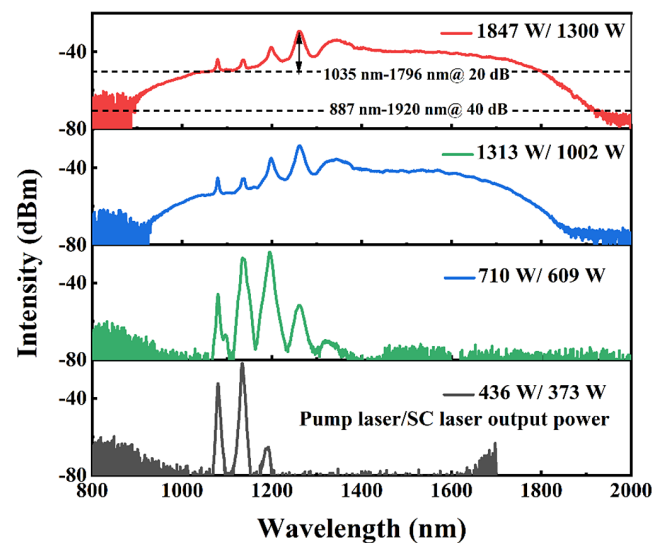


Figure 5. Output spectral evolution with pump laser power in the RFL with a half-open cavity.

In the following, the output performances of the RFL with a half-open cavity are analyzed in detail. Figure 5 presents the output spectral evolution. The mechanism of the initial spectrum expansion is similar to that of the full-opened RFL, which is dominated by the cascaded Raman effect. The modulation instability (MI) starts to work and gives birth to a train of ultra-short pulses when the long wavelength edge of the spectrum is extended beyond the ZDW of the fiber^[19]. In the short wavelength direction, the whole Raman substrate is connected under the combined action of dispersive waves trapped by soliton and phase-matched four-wave mixing^[20]. In the long wavelength direction, the extension of the spectrum is induced by the

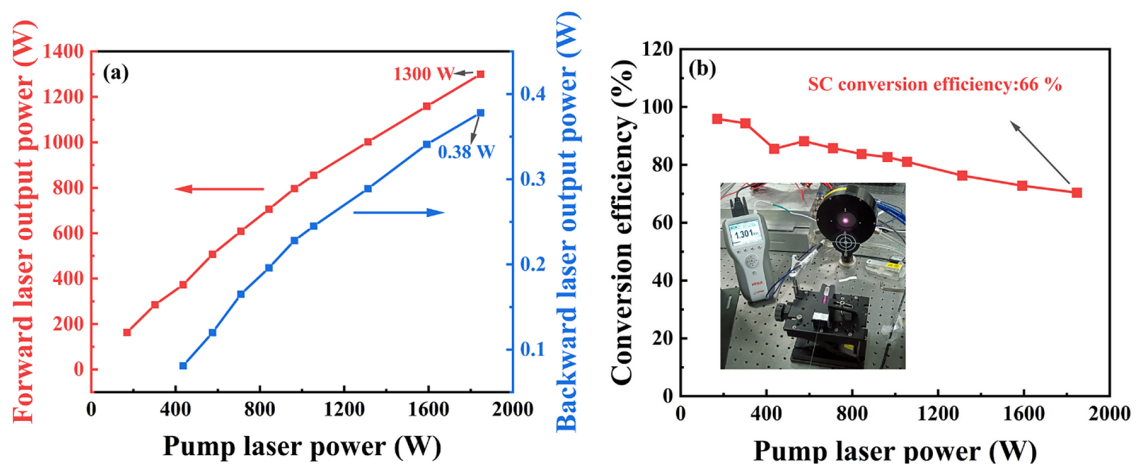


Figure 6. (a) Laser output power and (b) conversion efficiency in the RFL with a half-open cavity.

soliton self-frequency shift and soliton fission^[21]. With the further increasing pump power, these effects are stimulated more effectively and together enhance the broadening of spectrum. Although with the combination of the CW pump and the LMA fiber with a low nonlinear coefficient it is difficult to excite various nonlinear effects, the spectrum is broadened in effect, which benefits from the high pump power and the long interaction length of various nonlinear effects increased by random distributed feedback^[6]. When the pump power reaches 1847 W, a broadband spectrum covering 887–1920 nm is then obtained.

Figure 6 presents the laser output power and the conversion efficiency versus the pump laser power in the half-opened RFL. When the pump power reaches 1847 W, the SC output power reaches 1300 W. The conversion efficiency decreases with the increase of pump power due to the quantum defect occurring in the whole process of wavelength conversion. Concerning that for the final SC, the laser conversion efficiency reaches 66%, which is the highest conversion efficiency in a reported RFL output SC with the same spectral range. Such a high conversion efficiency is benefited by the introduced position of feedback in our structure. The feedback is introduced between the pump laser and the passive fiber, and thus the SC output power is difficult to increase and the SC output spectrum and conversion efficiency are also relatively poor (see the [supplementary material](#) for details). In our structure, the feedback is introduced before the pump laser, and the backward scattered light passes through the YDF and experiences the ytterbium ion gain in the bandwidth range of 1000–1200 nm. Then, both the 1000–1200 nm wavelength range backward light and the 1080 nm signal light extract energy from the 940 nm pump light, promoting the conversion of the pump light and enhancing the conversion efficiency. The bandwidth of the coupler is 1120–1200 nm. The light in the wavelength range will pass through the YDF multiple times due to the presence of the coupler with broadband strong feedback,

further enhancing this effect. In addition, the bandwidth of the coupler covers the strong radiation wavelengths of backward light (1134 nm backward first-order Raman and 1193 nm backward second-order Raman). The coupler is fabricated by the fused taper technique. The light located in the bandwidth of the coupler obtains strong feedback, and the light located outside the bandwidth of the coupler obtains relatively weak feedback. With the aid of the coupler, the backward light loss is reduced and the conversion efficiency is improved.

The temporal behaviors of the half-opened RFL are measured in the output end by an InGaAs photo-detector with a bandwidth of 1 GHz and an oscilloscope with a bandwidth of 1.5 GHz. The standard deviation (STD) values displayed are used to characterize the temporal dynamics. The results are shown in Figure 7. The RFL has the advantage of suppressing the self-pulsing effect^[22]. In self-pulsing dynamics, the photon lifetime in the cavity plays a major role. The longer the photon lifetime in the cavity τ_c , the more stable the time domain due to the suppression of self-pulsing. It can be calculated by the following formula^[23]:

$$\tau_c = \frac{2nL}{c(-\ln R_1 R_2 + 2\alpha l)}$$

where L is the length of the resonator, l is the length of the gain fiber, n is the refractive index of the fiber, R_1 and R_2 are the two-side reflectivities of the resonator and α is the scattering loss. The length of the gain fiber is relative to the pump light. It refers to the fact that when the length of the gain fiber is long, the saturable absorption effect in the weakly pumped portion of the gain fiber triggers a strong self-pulsing effect initiated by the relaxation oscillations, corresponding to the reduction of the intracavity photon lifetime in the formula^[23]. However, the length of the resonator is relative to the signal light. Concerning the

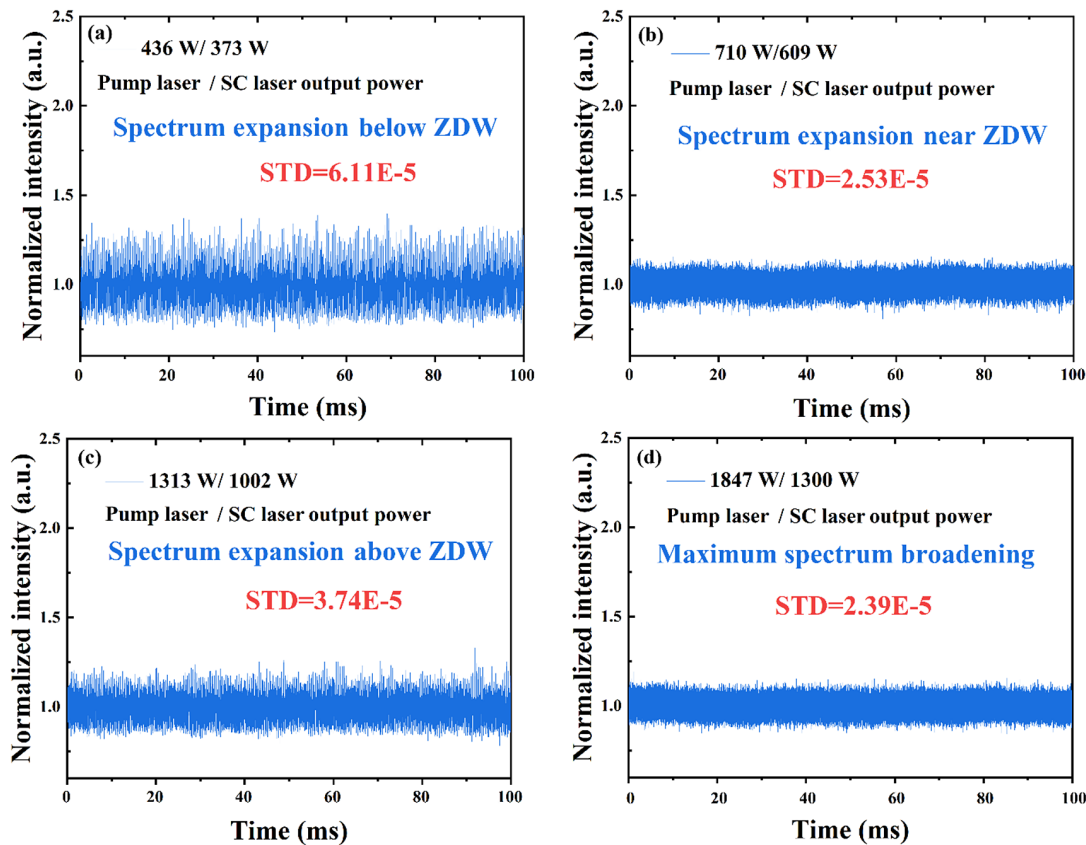


Figure 7. Normalized temporal signal of the RFL with a half-open cavity: (a) spectrum expansion below the ZDW; (b) spectrum expansion near the ZDW; (c) spectrum expansion above the ZDW; (d) maximum spectrum broadening. The recording time window is set to 100 ms.

cavity of the RFL, multiple scattering caused by random distributed feedback increases the length of the resonator, thus enhancing the photon lifetime in the cavity and leading to a stable CW operation^[24]. With the increase of pump power, Rayleigh scattered light based on random distributed feedback is strengthened. On the one hand, the part of the backward Rayleigh scattered light at 1080 nm is amplified in the oscillator, reducing the time domain fluctuation of the 1080 nm signal light, and the corresponding time domain properties are transferred from the signal light to subsequent Raman lights. On the other hand, the random distributed feedback of Raman light enhances the intracavity photon lifetime. Based on the above two aspects, a stable Raman laser output is obtained. As shown in Figures 7(a) and 7(b), the STD values indicate that the output laser becomes more and more stable with the increasing pump power during the whole conversion process of the Raman peak. When the spectrum extends beyond the ZDW of the fiber, a slight time domain fluctuation could be observed in Figure 7(c), which tends to be caused by nonlinear effects involving the process of SC broadening, such as soliton fission. Because the generated pulse originating from the soliton fission has random duration and energy, a pulse train with periodic modulation is not observed in the time domain. With the further increase of pump power, the time domain becomes

more stable again owing to the increasing intracavity photon lifetime caused by enhanced random distributed feedback, which is shown in Figure 7(d). The results indicate that this scheme could produce a stable SC laser source, especially during high-power operation.

4. Conclusion

In conclusion, a novel experimental scheme is used to realize kilowatt-level SC output. In the absence of feedback, the combination of Rayleigh scattering, distributed Raman gain and active gain results in a high-power backward laser output, which limits the power scaling of the forward laser. By introducing the feedback before the pump laser, the backward power loss can be reduced and the pump can be fully utilized, which improves the forward output power and conversion efficiency significantly. At the maximum pump power of 1847 W, a 1300 W SC with a spectrum covering 887–1920 nm and an optical conversion efficiency of 66% is obtained. The output temporal behaviors illustrate that the RFL cavity can stably work. Compared with the reported RFL output SC, the experimental structure is the simplest and the conversion efficiency is the highest in the same spectral range. This simple scheme not only can be used to generate a high-power SC laser with high efficiency

and sound robustness, but also presents rich phenomena, providing important reference significance for other lasers (such as Raman fiber lasers and point-reflector-free RFLs), as well as scientific research.

Acknowledgements

The work was supported by the Natural Science Foundation of Hunan Province (No. 2022JJ30653). The authors are grateful to Desheng Zhao, Lingfa Zeng, Xiaoyong Xu and Sen Guo for their help during the experiment.

Supplementary Material

To view supplementary material for this article, please visit <http://doi.org/10.1017/hpl.2023.66>.

References

1. J. C. Knight, T. A. Birks, P. S. J. Russell, and D. M. Atkin, *Opt. Lett.* **21**, 1547 (1996).
2. A. Manninen, T. Kaariainen, T. Parviainen, S. Buchter, M. Heilio, and T. Laurila, *Opt. Express* **22**, 7172 (2014).
3. H. Kawagoe, S. Ishida, M. Aramaki, Y. Sakakibara, E. Omoda, H. Kataura, and N. Nishizawa, *Biomed. Opt. Express* **5**, 932 (2014).
4. J. C. Knight, *Nature* **424**, 847 (2003).
5. L. Jiang, R. Song, J. He, and J. Hou, *Opt. Laser Technol.* **161**, 109168 (2023).
6. T. Qi, Y. Yang, D. Li, P. Yan, M. Gong, and Q. Xiao, *J. Lightwave Technol.* **40**, 7159 (2022).
7. L. Wang, H. Zhang, X. Xi, P. Wang, D. Zhang, B. Yang, C. Shi, X. Wang, and X. Xu, *Opt. Lett.* **47**, 5809 (2022).
8. S. A. Babin, E. I. Dontsova, and S. I. Kablukov, *Opt. Lett.* **38**, 3301 (2013).
9. Y. Wang, R. Kitahara, W. Kiyoyama, Y. Shirakura, T. Kurihara, Y. Nakanish, T. Yamamoto, M. Nakayama, S. Ikoma, and K. Shima, *Proc. SPIE* **11260**, 1126022 (2020).
10. H. Zhang, L. Huang, J. Song, H. Wu, P. Zhou, X. Wang, J. Wu, J. Xu, Z. Wang, X. Xu, and Y. Rao, *Opt. Lett.* **44**, 2613 (2019).
11. H. Zhang, J. Wu, Y. Wan, P. Wang, B. Yang, X. Xi, X. Wang, and P. Zhou, *Opt. Lett.* **47**, 493 (2022).
12. S. Arun, V. Choudhury, V. Balaswamy, R. Prakash, and V. R. Supradeepa, *Opt. Express* **26**, 7979 (2018).
13. K. Y. Lau, F. H. Suhailin, N. H. Z. Abidin, A. F. Abas, M. T. Alresheedi, and M. A. Mahdi, *IEEE Photonics J.* **11**, 1503707 (2019).
14. X. Cheng, J. Dong, X. Zeng, J. Zhou, S. Cui, W. Qi, Z. Lin, H. Jiang, and Y. Feng, *Opt. Laser Technol.* **68**, 102825 (2022).
15. S. Arun, V. Choudhury, V. Balaswamy, and V. R. Supradeepa, *Opt. Lett.* **45**, 1172 (2020).
16. X. Y. Ma, J. M. Xu, J. Ye, Y. Zhang, L. J. Huang, T. F. Yao, J. Y. Leng, Z. Y. Pan, and P. Zhou, *High Power Laser Sci. Eng.* **20**, e8 (2022).
17. I. Ilev, H. Kumagai, K. Toyoda, and I. Koprnikov, *Appl. Opt.* **35**, 2548 (1996).
18. I. D. Vatnik, D. V. Churkin, and S. A. Babin, *Opt. Express* **20**, 28033 (2012).
19. A. K. Abeeluck and C. Headley, *Opt. Lett.* **30**, 61 (2005).
20. J. C. Travers, A. B. Rulkov, B. A. Cumberland, S. V. Popov, and J. R. Taylor, *Opt. Express* **16**, 14435 (2008).
21. M. H. Frosz, O. Bang, and A. Bjarklev, *Opt. Express* **14**, 9391 (2006).
22. H. Zhang, L. Huang, P. Zhou, X. Wang, J. Xu, and X. Xu, *Opt. Lett.* **42**, 3347 (2017).
23. B. N. Upadhyaya, A. Kuruvilla, U. Chakravarty, M. R. Shenoy, K. Thyagarajan, and S. M. Oak, *Appl. Opt.* **49**, 2316 (2010).
24. R. Ma, J. Liu, Z. Q. Fang, and D. Y. Fan, *J. Lightwave Technol.* **39**, 5089 (2021).